Neoplasma 2025; 72(4): 253–261

doi:10.4149/neo_2025_250509N199

N6-methyladenosine-induced hsa_circ_0011536 acts as a microRNA-576-5p sponge to promote ferroptosis of non-small cell lung cancer cells via transferrin receptor

Junming HUANG[1,#], Caijiu DENG[2,3,#,*], Hanhan ZHU[4,#], Xiaofeng CHEN[5], Peixi CHEN[1], Shaoshan DU[1]

[1]Department of Oncology, Panyu Hospital of Traditional Chinese Medicine, Panyu Hospital Guangzhou University of Chinese Medicine, Guangzhou, China; [2]Department of Oncology, The Affiliated Panyu Central Hospital, Guangzhou Medical University, Guangzhou, China; [3]Cancer Institute of Panyu District,The Affiliated Panyu Central Hospital,Guangzhou Medical University; [4]The Sixth Affiliated Hospital of Jinan University, Dongguan, China; [5]Department of Orthopedics, Panyu Hospital of Traditional Chinese Medicine, Panyu Hospital Guangzhou University of Chinese Medicine, Guangzhou, China

**Correspondence: dengcaijiu@pyhospital.com.cn*
[#]Contributed equally to this work.

Received May 9, 2025 / Accepted August 4, 2025

Lung cancer is the leading cause of death and the most diagnosed cancer worldwide. Non-small cell lung cancer (NSCLC) is the most common type of lung cancer; 85% of lung cancer patients are diagnosed with NSCLC. Though numerous treatments for lung cancer have been developed, the 5-year survival rate of patients with NSCLC remains low. Therefore, it is urgent to explore novel targets for NSCLC treatment. Growing evidence has revealed that circular RNAs (circRNAs) contribute to NSCLC progression. Besides, the data of circRNA microarray (GSE158695) has found that hsa_circ_0011536 is downregulated in NSCLC tissues. Nevertheless, the role of hsa_circ_0011536 in NSCLC remains unknown. In this study, RNA 6-methyladenosine (m^6A) modification was detected by methylated RNA immunoprecipitation, the interaction of RNAs was determined using miRNA pulldown and luciferase reporter assay, while ferroptosis was identified by Cell Counting Kit-8 assay, intracellular iron content, and malondialdehyde level. Our findings demonstrated that hsa_circ_0011536 was downregulated in NSCLC cell lines. Mechanism investigation revealed that m^6A modification enhanced the back-splicing of pre-ZMYM4 to increase hsa_circ_0011536 expression in A549 and NCI-H1299 cells. Moreover, hsa-miR-576-5p was the target of hsa_circ_0011536, while transferrin receptor (TFRC) was the downstream target of hsa-miR-576-5p in A549 and NCI-H1299 cells. Furthermore, hsa_circ_0011536 elevated TFRC expression by sponging hsa-miR-576-5p in A549 and NCI-H1299 cells, identified by luciferase reporter assay. In addition, hsa_circ_0011536 induced ferroptosis through hsa-miR-576-5p in A549 and NCI-H1299 cells. Therefore, this study revealed that m^6A-induced hsa_circ_0011536 elevated TFRC expression to induce ferroptosis by sponging hsa-miR-576-5p in NSCLC. These results might provide novel therapeutic targets for NSCLC treatment.

Key words: non-small cell lung cancer; RNA methylation; hsa_circ_0011536; hsa-miR-576-5p; miRNA sponge; ferroptosis

Lung cancer is the leading cause of death and the most diagnosed cancer worldwide [1–3]. It is estimated that around 2 million new cases of lung cancer occur and 1.6 million patients with lung cancer die annually [3, 4]. Non-small cell lung cancer (NSCLC) is the most common type of lung cancer; 85% of lung cancer patients are diagnosed with NSCLC [5]. Most lung cancer patients have advanced stage disease (stage III or IV) at initial diagnosis [4]. Thus, though numerous treatments for lung cancer have been developed, including thoracic surgery, radical radiotherapy, microwave ablation, cancer immunotherapy, and targeted therapy [6, 7], the 5-year survival rate of patients with NSCLC varies only from 4–17% depending on stages [4]. It is urgent to explore novel targets for NSCLC treatment.

As novel endogenous non-coding RNAs, circRNAs are covalently connected to the structure of a closed-loop by back-splicing processes from pre-mRNAs [8, 9]. It has been reported that circRNAs play numerous critical roles, such as nuclear transcription regulators, microRNA (miRNA) sponges, and protein sponges [10–14]. More importantly, circRNAs contribute to NSCLC progression. For instance, circNDUFB2 activates anti-tumor immunity through

degrading IGF2BPs to suppress NSCLC progression [15]. By contrast, circSATB2 upregulates fascin homolog 1, actin-bundling protein 1 (FSCN1) expression by sponging miR-326 to promote NSCLC progression [16]. However, the knowledge of the effects of circRNAs on NSCLC progression is still limited. The data of circRNA microarray (GSE158695) from a previous study have shown that hsa_circ_0011536 is dramatically downregulated in NSCLC tissues [15]. Nevertheless, the role of hsa_circ_0011536 in NSCLC remains unknown.

RNA methylation contributes to the occurrence and development of NSCLC by regulating transportation, localization, stability, shearing, and translation of RNAs [17–20]. To date, N6-methyladenosine (m^6A) is the most abundant modification among RNA methylation [21]. Some studies have indicated that m^6A modification could regulate circRNA expression by modifying the back-splicing process. For instance, m^6A modification facilitates the generation of circ1662 by enhancing back-splicing in colorectal cancer [22]. Besides, m^6A modification promotes the back-splicing of pre-METTL3 mRNA to increase circMETTL3 expression in breast cancer [23]. Nevertheless, the effect of m^6A modification on hsa_circ_0011536 expression in NSCLC has not been reported.

Previous studies have revealed that circRNAs regulate NSCLC progression as miRNA sponges. For example, circSATB2 upregulates FSCN1 expression by sponging miR-326 to facilitate NSCLC progression [16]. Besides, circ-CPA4 activates programmed cell death ligand 1 (PD-L1) axis to promote growth, immune evasion, drug resistance, and stemness of NSCLC through sponging let-7 [24]. However, miRNAs regulated by hsa_circ_0011536 are largely unknown.

Ferroptosis is a novel iron-dependent programmed cell death, which exerts an active effect on suppressing NSCLC progression [13, 25, 26]. Some studies have demonstrated that circRNAs regulate ferroptosis through miRNAs in cancers. For instance, circRHOT1 prohibits ferroptosis through miR-106a-5p in breast cancer [27]. Besides, circ_0067934 inhibits ferroptosis by sponging miR-545-3p to activate the ferroptosis-negative regulator solute carrier family 7 member 11 (SLC7A11) in thyroid cancer [28]. To date, only one study has reported that circDTL suppresses ferroptosis by miR-1287-5p to upregulate the ferroptosis-negative regulator glutathione peroxidase 4 (GPX4) expression in NSCLC [29]. Thus, the roles of circRNAs, including hsa_circ_0011536, in ferroptosis of NSCLC remain unclear.

Therefore, the primary aim of this study was to investigate whether m^6A modification regulated hsa_circ_0011536 expression and hsa_circ_0011536 induced ferroptosis through miRNA in NSCLC.

Materials and methods

Cell culture. NSCLC cell lines, including A549, SK-MES-1, and NCI-H1299 cells, and normal human alveolar epithelial type II (AT2) cells were obtained from the Cell Bank at the Chinese Academy of Sciences (Shanghai, China). Cells were cultured in RPMI-1640 medium (Hyclone, South Logan, UT, USA) containing penicillin-streptomycin (100 U/ml, Hyclone) and fetal bovine serum (FBS, 10%, Hyclone) in a humidified incubator with 5% CO_2 at 37 °C.

Cell transfection. hsa_circ_0011536 expression vector, blank expression vector, hsa-miR-576-5p mimic, mimic negative control (NC), biotin-labeled hsa-miR-576-5p pulldown probe, NC probe, FTO alpha-ketoglutarate dependent dioxygenase (FTO) siRNA and siRNA NC obtained from Hytran Biotech (Guangzhou, Guangdong, China) were transfected into A549 and NCI-H1299 cells by Lipofectamine 2000 (Invitrogen, Carlsbad, CA, USA) according to the manufacturer's instructions. After transfection for 48 h, cells were collected and used for the subsequent experiments. The siRNAs used in this study were as follows: FTO sense: 5'-AUAGCAGUCUCCUUGGUGA-3', antisense: 5'-ACCAAGGAGACUGCUAUUU-3'; siRNA NC sense: 5'-UUCUCCGAACGUGUCACGU-3', antisense: 5'-ACGUGACACGUUCGGAGAA-3'.

Quantitative reverse transcription-PCR (qRT-PCR). Total RNA from A549, SK-MES-1, NCI-H1299, and AT2 cells was extracted using TRIzol (Invitrogen, USA). Next, reverse transcription of RNA to cDNA was performed using PrimeScript™ II 1st Strand cDNA Synthesis Kit (TaKaRa Biotechnology, Dalian, Liaoning, China) according to the manufacturer's instructions. Subsequently, qRT-PCR was performed by TB Green® Premix Ex Taq™ (Tli RNaseH Plus) (Takara Biotechnology). Then the amount of target RNA was normalized to the amount of internal control (GAPDH), and the results were given by $2^{-\Delta\Delta Ct}$ relative to the control sample. The primers used in this study were as follows: hsa_circ_0011536 forward: 5'-GGGATTCCAGCTACCCATTT-3', reverse: 5'-GCTGTCAAGGGTAGGAGTTAAG-3'; TFRC forward: 5'-CGCTGGTCAGTTCGTGATTA-3',reverse:5'-CTGGAAGTAGCACGGAAGAAG-3'; pre- zinc finger MYM-type containing 4 (ZMYM4) forward: 5'-CACACAGCATGAATCAGACAATG-3', reverse: 5'-TTTCACGTTCATAAGTTAGGTCTCT-3'; FTO forward: 5'-ACACACCGAGGCTGAAATAG-3', reverse: 5'-CTTCATCTTGTCCGTTGTAGGA-3'; GAPDH forward: 5'-AACGGATTTGGTCGTATTGGG-3', reverse: 5'-CCTGGAAGATGGTGATGGGAT-3'.

Bioinformatics analysis. m^6A sites on hsa_circ_0011536 were predicted by RMVar v2.0 (https://rmvar.renlab.cn/#/home). Besides, targeted miRNAs of hsa_circ_0011536 were dug using CircRNA Interactome (https://circinteractome.nia.nih.gov/). Moreover, TargetScan (www.targetscan.org/) was utilized to explore the downstream target of hsa-miR-576-5p.

Methylated RNA Immunoprecipitation (MeRIP). MeRIP was performed using the MeRIP Kit purchased from Hytran Biotech. Briefly, AT2, A549, and NCI-H1299 cells were collected and lysed, followed by the interruption

of RNA using the RNA fragmentation Buffer according to the manufacturer's procedures. Then, the cell lysate was incubated with m^{6}A-specific antibody at 4 °C overnight. Subsequently, m^{6}A-specific antibody and m^{6}A-modified RNA fragments were captured by avidin magnetic beads, and the level of m^{6}A-modified RNA was identified by qRT-PCR.

miRNA pulldown. First, biotin-labeled hsa-miR-576-5p pulldown probe (AUUCUAAUUUCUCCACGUCUUU) and NC pulldown probe were synthesized by Hytran Biotech. Then, probes were transfected into A549 and NCI-H1299 cells using Lipofectamine 2000 (Invitrogen). After transfection, cells were collected by centrifugation and treated with lysis buffer, and 20 μl of cell supernatant was collected as input. Next, for the precipitate, magnetic beads (Thermo Fisher Scientific) were incubated with biotinylated hsa-miR-576-5p or NC probes to generate probe-coated beads, followed by incubation with cell lysates at 4 °C overnight. Subsequently, the RNAs associated with the beads were collected and purified. Then the abundance of hsa_circ_0011536, TFRC mRNA, or GAPDH in bound fractions was determined by qRT-PCR.

Western blot (WB). Total proteins were extracted from A549, SK-MES-1, NCI-H1299, and AT2 cells using RIPA buffer (Cell Signaling Technology, Danvers, MA, USA), and the concentration of proteins was quantified by BCA Protein Quantification Kit (Abbkine, Wuhan, Hubei, China). Then the same amount of protein was separated by SDS-PAGE and transferred to PVDF membranes (Millipore, Bedford, MA, USA), and then the PVDF membranes were incubated with 5% milk followed by primary antibodies at 4 °C overnight. Next, PVDF membranes were washed with Tris-Buffered Saline (TBS) and incubated with corresponding second antibodies (SouthernBiotech, Birmingham, AL, USA) at room temperature (RT) for 1 h. Subsequently, PVDF membranes were visualized by Chemiluminescence Detection Kit (Beyotime, Shanghai, China). The primary antibodies used in this study included TFRC (1:1000, #PAB171Hu01, USCN, Wuhan, Hubei, China) and GAPDH (1:10000, #KC-5G5, KangCheng, Shanghai, China).

Luciferase reporter assay. The wild type (WT) 3'UTR region of TFRC mRNA containing the putative binding site with hsa-miR-576-5p was amplified by PCR and cloned into pmirGLO luciferase reporter vector (Hytran Biotech). To construct the hsa_circ_0011536 expression vector, the cDNA sequence of hsa_circ_0011536 (755 bp) was obtained by PCR amplification using the following primers: hsa_circ_0011536-OE forward: 5'-CCCTTCTCAAGACGGATCCGTGGTGGTATCATGGATACAGAAATGTCTGAA-3', reverse: 5'-TTGAGCTCTCCACTCGAATTCTTGAGCATTGTCAGGTTCATCTTTTATTTTGTCTAGTA-3', and then cloned into the PcircRNA-hsa vector (Hytran Biotech). Then the luciferase reporter plasmids were co-transfected with hsa-miR-576-5p mimics, mimics NC, hsa_circ_0011536 expression vector, or blank expression vector into A549 cells and NCI-H1299 cells using Lipofectamine 2000 (Invitrogen). Following 48 h transfection, relative luciferase activity was determined using the Dual-Luciferase Reporter Assay System (Promega, Madison, WI, USA) with Renilla luciferase activity as the internal control.

CCK-8 assay. Cell proliferation was evaluated by using the cell counting kit-8 assay (Beyotime) according to the manufacturer's instructions. In brief, A549 cells and NCI-H1299 cells were seeded into 96-well plates. Following 0 h, 24 h, 48 h and 72 h transfection of hsa_circ_0011536 expression vector, blank expression vector, hsa-miR-576-5p mimics or mimics NC, 10 μl CCK-8 solution was added to incubate cells for 4 h, then the absorbance was detected by the Multiscan MK3 microplate reader (Thermo Fisher Scientific, Waltham, MA, USA) at 450 nm.

Determination of intracellular iron content. Intracellular iron content was evaluated by using the Iron Colorimetric Assay Kit (Applygen, Beijing, China) following the manufacturer's protocol. In brief, A549 cells and NCI-H1299 cells were seeded into 96-well plates. Following 48 h transfection of hsa_circ_0011536 expression vector, blank expression vector, hsa-miR-576-5p mimics or mimics NC, cells were collected for detection. The absorbance of cells was detected by a Multiscan MK3 microplate reader (Thermo Fisher Scientific) at 550 nm.

Statistical analysis. All data in this study were obtained from three replicates and presented as mean ± SD. All experiments were repeated three times. Statistical differences were determined by Student's t-test (two groups) or post-hoc Tukey's test following one-way ANOVA (multiple groups) using SPSS software (v20, SPSS Inc., Chicago, IL, USA). A p-value <0.05 was considered a significant threshold.

Results

hsa_circ_0011536 is downregulated in NSCLC tissues and cell lines. The data of circRNA microarray (GSE158695) from a previous study have shown that hsa_circ_0011536 is dramatically downregulated in NSCLC tissues compared to that in non-cancer normal tissues (Figure 1A). Besides, the level of hsa_circ_0011536 was also detected in several NSCLC cell lines by qRT-PCR. Results found that the level of hsa_circ_0011536 was significantly decreased in NSCLC cell lines, including A549, SK-MES-1, and NCI-H1299 cells, compared to that in AT2 cells (Figure 1B). These results suggested that hsa_circ_0011536 was downregulated in NSCLC tissues and cell lines. Moreover, A549 and NCI-H1299 cells were utilized in the following experiments, as the hsa_circ_0011536 level in A549 and NCI-H1299 cells declined more than that in SK-MES-1 cells.

m^{6}A modification increases hsa_circ_0011536 expression in A549 and NCI-H1299 cells. Next, the mechanism regulating hsa_circ_0011536 expression in NSCLC was investigated. Bioinformatics analysis showed that there were two potential m^{6}A sites near the back-splicing junction of hsa_circ_0011536 (Figure 2A), suggesting that m^{6}A modifi-

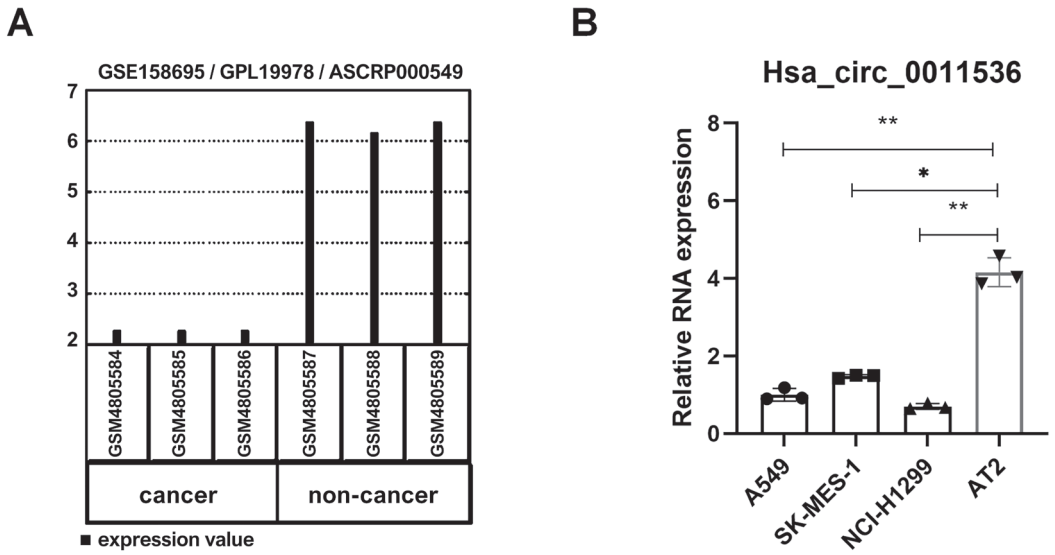

Figure 1. hsa_circ_0011536 is downregulated in NSCLC tissues and cell lines. A) The level of hsa_circ_0011536 in NSCLC tissues and non-cancer normal tissues. B) The level of hsa_circ_0011536 in A549, SK-MES-1, NCI-H1299, and AT2 cells. N=3 replicates. *p<0.05, **p<0.01, ***p<0.001

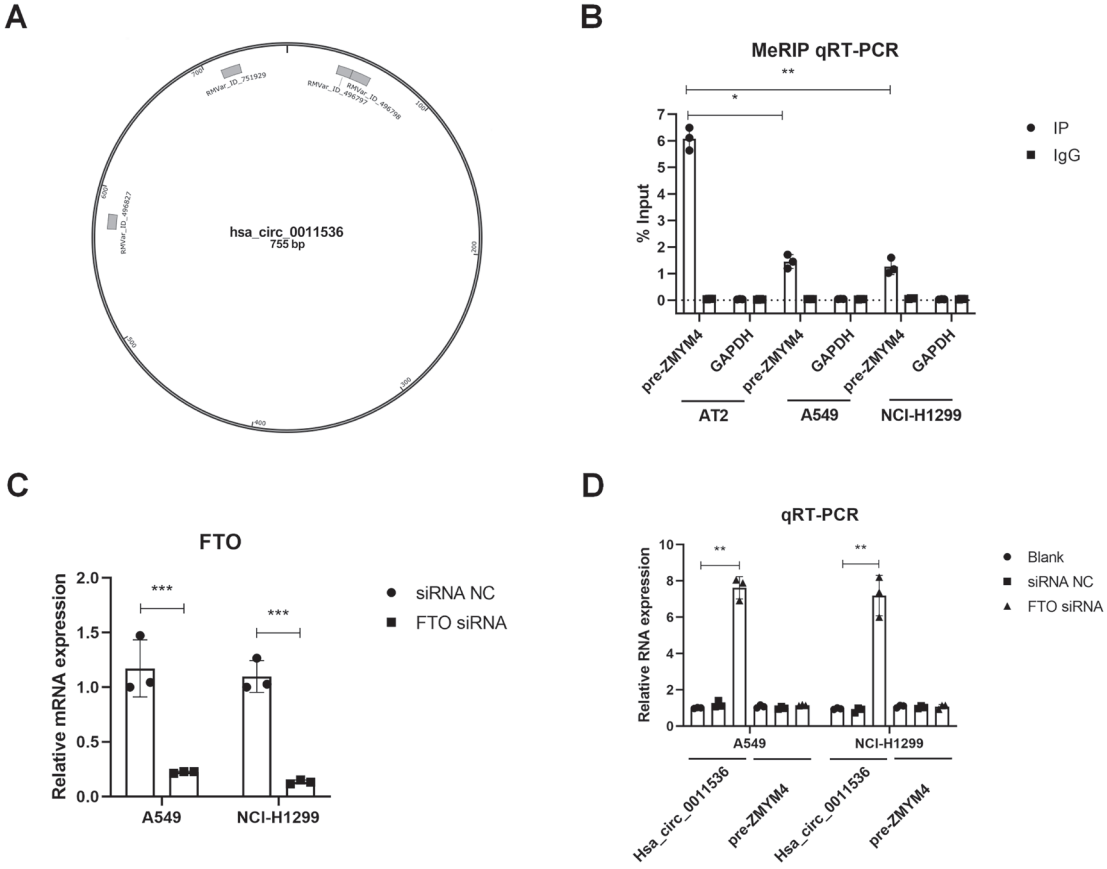

Figure 2. m⁶A modification enhanced the back-splicing of pre-ZMYM4 to increase hsa_circ_0011536 expression in A549 and NCI-H1299 cells. A) The potential m⁶A sites in hsa_circ_0011536. B) The m⁶A modification level of pre-ZMYM4 detected by MeRIP in A549 and NCI-H1299 cells. C) FTO mRNA level in A549 and NCI-H1299 cells treated with or without FTO siRNA. D) Levels of hsa_circ_0011536 and pre-ZMYM4 in A549 and NCI-H1299 cells treated with or without FTO siRNA. Abbreviation: NC-negative control; N=3 replicates. *p<0.05, **p<0.01, ***p<0.001

cation might contribute to the back-splicing progress of hsa_circ_0011536.

As hsa_circ_0011536 derives from *ZMYM4*, the m^{6}A modification level of pre-ZMYM4 was detected by MeRIP. Results indicated that the m^{6}A modification level of pre-ZMYM4 was significantly decreased in A549 and NCI-H1299 cells compared to that in AT2 cells (Figure 2B). Subsequently, m^{6}A demethylase FTO was silenced by siRNA in A549 and NCI-H1299 cells (Figure 2C), and levels of pre-ZMYM4 and hsa_circ_0011536 were detected using qRT-PCR. It was shown that FTO silence elevated hsa_circ_0011536 level in A549 and NCI-H1299 cells (Figure 2D), while FTO silence had no effect on pre-ZMYM4 level in A549 and NCI-H1299 cells (Figure 2D). Therefore, the above results suggested that m^{6}A modification enhanced the back-splicing of pre-ZMYM4 to increase hsa_circ_0011536 expression in A549 and NCI-H1299 cells.

hsa-miR-576-5p is the targeted miRNA of hsa_circ_0011536 in A549 and NCI-H1299 cells. Then targeted miRNAs of hsa_circ_0011536 in NSCLC were explored. Bioinformatic analysis by CircRNA Interactome found that hsa-miR-576-5p was a potential targeted miRNA of hsa_circ_0011536 (Figure 3A). Furthermore, results of miRNA pulldown demonstrated that hsa-miR-576-5p associated with hsa_circ_0011536 in A549 and NCI-H1299 cells (Figures 3B, 3C). The above data suggested that hsa-miR-576-5p was the target of hsa_circ_0011536 in A549 and NCI-H1299 cells.

TFRC is the downstream target of hsa-miR-576-5p in A549 and NCI-H1299 cells. Subsequently, TargetScan was utilized to investigate the downstream target of hsa-miR-576-5p in NSCLC. Bioinformatic analysis indicated that TFRC should be the potential target of hsa-miR-576-5p (Figure 3A). TFRC is a recognized inducer of ferroptosis [26, 30, 31]. Besides, miRNA pulldown revealed that hsa-miR-576-5p associated with TFRC mRNA in A549 and NCI-H1299 cells (Figures 3B, 3C). Thus, TFRC was the downstream target of hsa-miR-576-5p in A549 and NCI-H1299 cells.

hsa_circ_0011536 elevates TFRC expression through sponging hsa-miR-576-5p in A549 and NCI-H1299 cells. The TFRC expression was detected in several NSCLC cell lines by qRT-PCR and WB. Results showed that both TFRC mRNA level and protein level were downregulated in NSCLC cell lines, including A549, SK-MES-1, and NCI-H1299 cells, compared to those in normal human AT2 cells (Figures 4A, 4B). Therefore, the expression pattern of TFRC was similar to that of hsa_circ_0011536 in A549 and NCI-H1299 cells.

Subsequently, the luciferase activity of A549 and NCI-H1299 cells transfected with reporter gene vectors containing the binding site of hsa-miR-576-5p on 3' UTR of TFRC mRNA was decreased by the co-transfection of hsa-miR-576-5p mimic, whereas co-transfection of hsa_circ_0011536 expression vector reversed the effect of hsa-miR-576-5p mimic (Figures 4C, 4D). Besides, transfection of a blank expression vector had no effect on the luciferase activity of A549 and NCI-H1299 cells (Figures 4C, 4D).

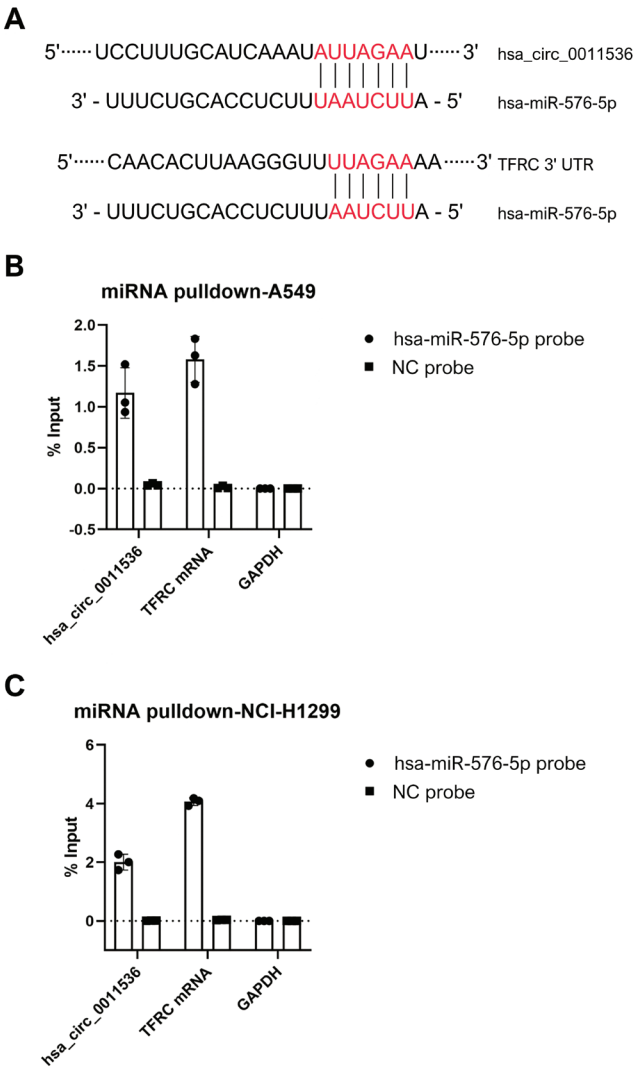

Figure 3. hsa-miR-576-5p is the targeted miRNA of hsa_circ_0011536, while TFRC is the downstream target of hsa-miR-576-5p in A549 and NCI-H1299 cells. A) The binding site of hsa-miR-576-5p in hsa_circ_0011536 and the binding site of hsa-miR-576-5p in TFRC mRNA 3'UTR region. B) miRNA pulldown and qPCR analysis of the association between hsa_circ_0011536 and hsa-miR-576-5p or the interaction of hsa-miR-576-5p and TFRC mRNA in A549 cells. C) miRNA pulldown and qPCR analysis of the association between hsa_circ_0011536 and hsa-miR-576-5p or the interaction of hsa-miR-576-5p and TFRC mRNA in NCI-H1299 cells. Abbreviation: NC-negative control; N=3 replicates.

Thus, these data together suggested that TFRC was the target of hsa-miR-576-5p, and hsa_circ_0011536 elevated TFRC expression by sponging hsa-miR-576-5p in A549 and NCI-H1299 cells.

hsa_circ_0011536 induces ferroptosis through hsa-miR-576-5p in A549 and NCI-H1299 cells. To further identify whether hsa_circ_0011536 induced ferroptosis in NSCLC through hsa-miR-576-5p, hsa_circ_0011536 expression vector and hsa-miR-576-5p mimic were utilized.

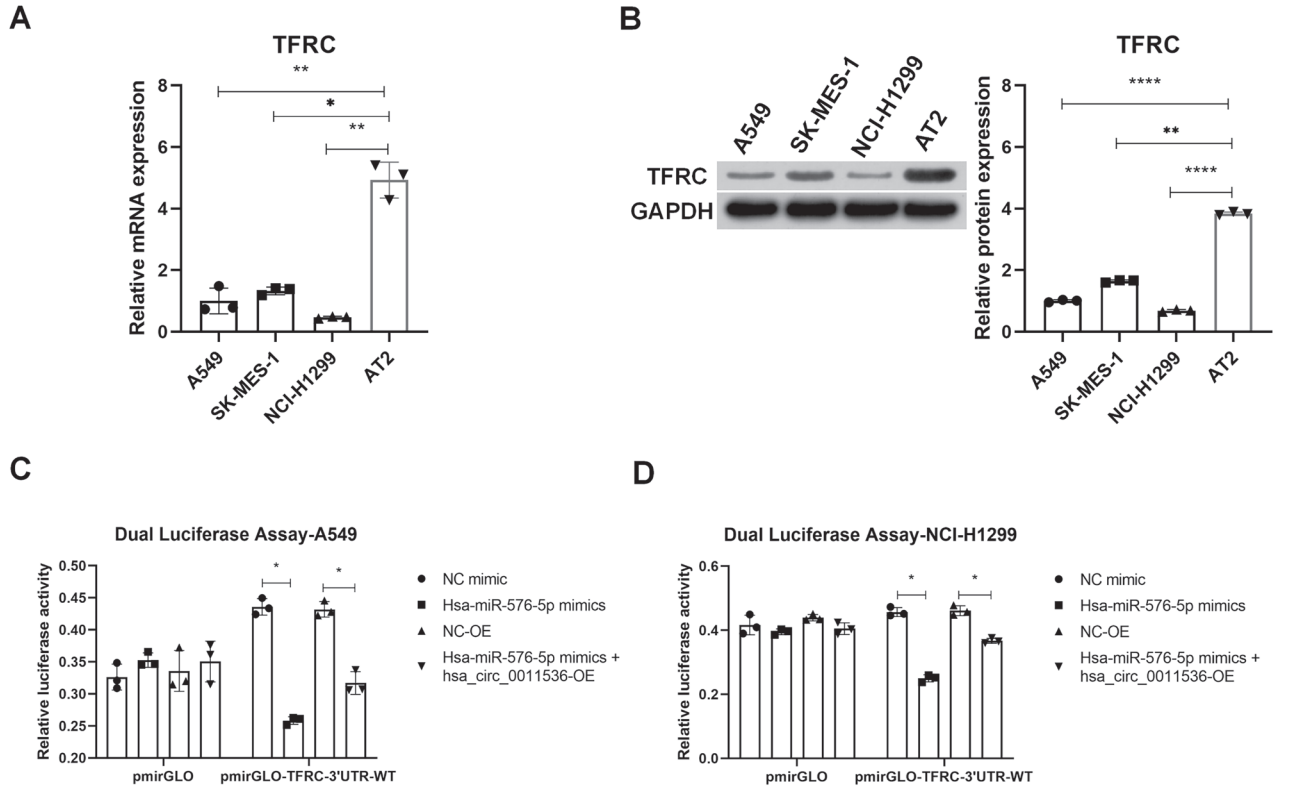

Figure 4. hsa_circ_0011536 elevates TFRC expression through sponging hsa-miR-576-5p in A549 and NCI-H1299 cells. A) The level of TFRC mRNA in A549, SK-MES-1, NCI-H1299, and AT2 cells. B) The level of TFRC protein in A549, SK-MES-1, NCI-H1299, and AT2 cells. C) Luciferase activity of A549 cells co-transfected with reporter gene vectors containing the binding site of hsa-miR-576-5p on TFRC mRNA 3' UTR region and hsa_circ_0011536 expression vectors or hsa-miR-576-5p mimics. D) Luciferase activity of NCI-H1299 cells co-transfected with reporter gene vectors containing the binding site of hsa-miR-576-5p on TFRC mRNA 3' UTR region and hsa_circ_0011536 expression vectors or hsa-miR-576-5p mimics. Abbreviations: OE-overexpression; WT-wild type. N=3 replicates. *p<0.05, **p<0.01, ****p<0.0001

First, cell proliferation was detected by CCK-8 assay. Results showed that overexpression of hsa_circ_0011536 inhibited the proliferation of A549 cells and NCI-H1299 cells, whereas hsa-miR-576-5p overexpression abolished the effect of overexpression of hsa_circ_0011536 on the proliferation of A549 and NCI-H1299 cells (Figures 5A, 5B).

Next, markers of ferroptosis, including intracellular iron content and MDA level, were detected by ELISA. Results found that overexpression of hsa_circ_0011536 increased intracellular iron and MDA level in A549 and NCI-H1299 cells (Figure 5C, 5D). Besides, hsa-miR-576-5p overexpression reduced hsa_circ_0011536-elevated intracellular iron and MDA level in A549 cells and NCI-H1299 cells (Figure 5C, 5D). Taken together, the above results suggested that hsa_circ_0011536 induced ferroptosis through hsa-miR-576-5p in A549 and NCI-H1299 cells.

Discussion

This study revealed that hsa_circ_0011536 was downregulated in NSCLC cell lines. Mechanism investigation revealed that m^{6}A modification enhanced the back-splicing of pre-ZMYM4 to increase hsa_circ_0011536 expression in A549 and NCI-H1299 cells. Besides, hsa-miR-576-5p was the target of hsa_circ_0011536, while TFRC was the downstream target of hsa-miR-576-5p in A549 and NCI-H1299 cells. Moreover, hsa_circ_0011536 elevated TFRC expression by sponging hsa-miR-576-5p in A549 and NCI-H1299 cells. Furthermore, hsa_circ_0011536 induced ferroptosis through hsa-miR-576-5p in A549 and NCI-H1299 cells.

To date, the functional effects of hsa_circ_0011536 are largely unknown. Only one study has revealed that hsa_circ_0011536 might be an innovative predictor for the prognosis of colorectal cancer (CRC) [32]. Therefore, this study revealed the functional effect of hsa_circ_0011536 on ferroptosis for the first time.

Our findings revealed that m^{6}A modification enhanced the back-splicing of pre-ZMYM4 to increase hsa_circ_0011536 expression in NSCLC. However, the mechanism of m^{6}A modification regulating the back-splicing progress of pre-ZMYM4 to increase hsa_circ_0011536 expression was not explored in this study. A recent study has demonstrated

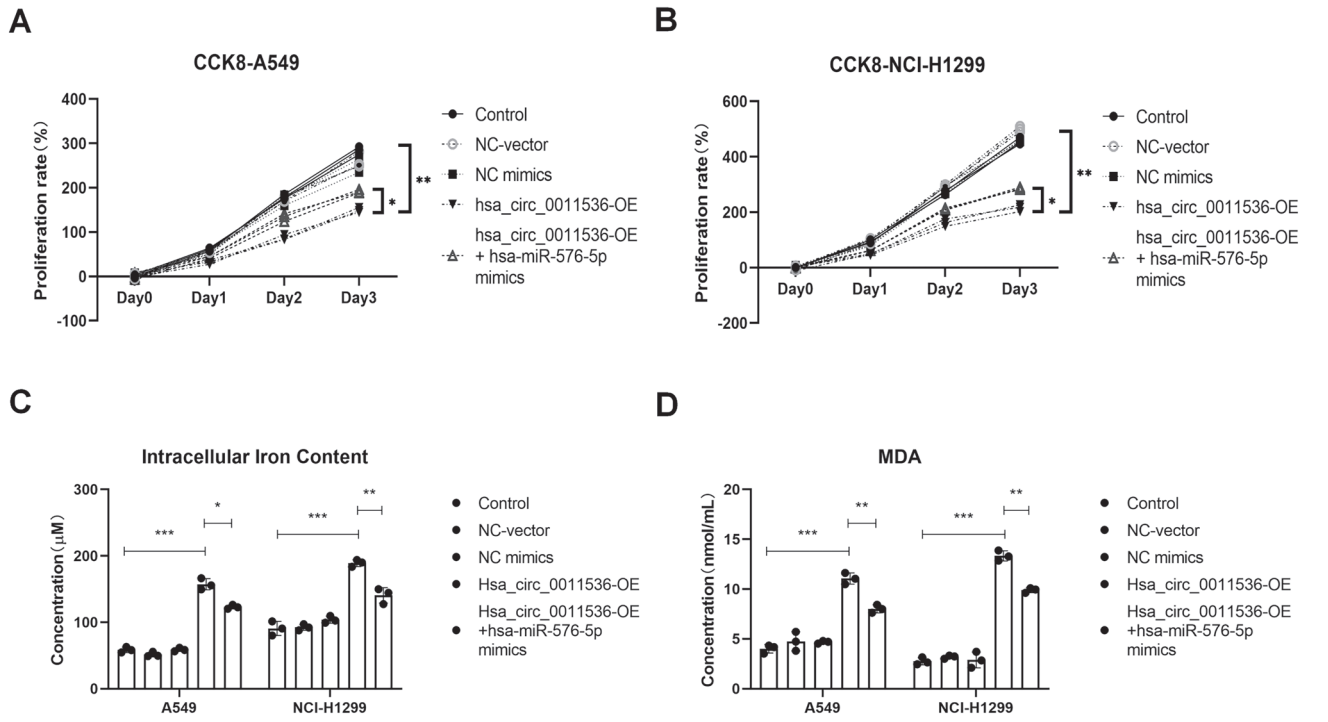

Figure 5. hsa_circ_0011536 induces ferroptosis through hsa-miR-576-5p in A549 and NCI-H1299 cells. A) The growth rate of A549 cells transfected with hsa_circ_0011536 expression vectors or hsa-miR-576-5p mimics. B) The growth rate of NCI-H1299 cells transfected with hsa_circ_0011536 expression vectors or hsa-miR-576-5p mimics. C) The intracellular iron content of A549 and NCI-H1299 cells transfected with hsa_circ_0011536 expression vectors or hsa-miR-576-5p mimics. D) The MDA level in A549 and NCI-H1299 cells transfected with hsa_circ_0011536 expression vectors or hsa-miR-576-5p mimics. Abbreviations: OE-overexpression; NC-negative control. N = 3. *p<0.05, **p<0.01, ***p<0.001

that DEAD-box helicase 5 (DDX5) binds to m^{6}A-modified pre-mRNAs by interacting with m^{6}A reader YTH N6-methyladenosine RNA binding protein C1 (YTHDC1) and facilitates the back-splicing process of pre-mRNAs to generate circRNAs [33]. Thus, m^{6}A modification might enhance the back-splicing reaction of pre-ZMYM4 to increase hsa_circ_0011536 expression through the YTHDC1/DDX5 axis in NSCLC.

Several studies have demonstrated the role of hsa-miR-576-5p in cancers. For instance, hsa-miR-576-5p might enhance the metastasis of CRC by targeting Wnt family member 5A [34]. Besides, long non-coding RNA (lncRNA) linc-PINT suppresses esophageal cancer progression through sponging hsa-miR-576-5p [35]. Moreover, hsa-miR-576-5p promotes the metastasis of esophageal squamous cell carcinoma cells via decreasing nuclear receptor-interacting protein expression [36]. However, the role of hsa-miR-576-5p in NSCLC remains unknown, and the present study uncovered the effect of hsa-miR-576-5p in NSCLC for the first time. Consistent with the role of hsa-miR-576-5p in other cancers, hsa-miR-576-5p also exerted oncogenic effects on NSCLC through inhibiting ferroptosis.

It has been reported that circRNAs play numerous critical roles, including miRNA sponges [10, 12-14]. Some studies have uncovered circRNAs regulating hsa-miR-576-5p. hsa_circ_0001666 inhibits CRC progression through upregulating protocadherin 10 as a sponge of hsa-miR-576-5p [37]. Besides, circ_0037078 enhances the growth, migration, invasion, and angiogenesis of trophoblast cells by sponging miR-576-5p [38]. However, the effect of hsa_circ_0011536 on hsa-miR-576-5p has not been studied. Thus, our study revealed the regulatory effect of hsa_circ_0011536 on hsa-miR-576-5p for the first time.

TFRC is a recognized inducer of ferroptosis [30, 31]. Previous studies have revealed that TFRC could be regulated by miRNAs. For example, hsa-miR-144-3p suppresses TFRC expression in glioma [39]. Besides, miR-378g facilitates the growth and mobility of laryngeal cancer cells by targeting TFRC [40]. Nevertheless, the regulatory effect of hsa-miR-576-5p on TFRC is largely unknown. Therefore, this study also revealed the regulatory effect of hsa-miR-576-5p on TFRC for the first time.

Additionally, there were some limitations of this study. For example, this study could be strengthened by identifying the mechanism of m^{6}A modification regulating the back-splicing of pre-ZMYM4 to increase hsa_circ_0011536 expression. Besides, the findings of the current study should be confirmed by *in vivo* experiments. Moreover, patient samples

with relevant clinical details should be involved to enhance transparency and reproducibility. Additionally, comparative treatments or controls would be used to assess the effectiveness of targeting hsa_circ_0011536. Our future studies will be committed to solving the above limitations.

In summary, this study revealed that m^{6}A-induced hsa_circ_0011536 elevated TFRC expression to induce ferroptosis by sponging hsa-miR-576-5p in NSCLC. These results might provide novel therapeutic targets for NSCLC treatment.

Acknowledgments: This work was supported by the General Medical and Health Projects of Panyu District Science and Technology Plan (2022-Z04-089).

References

[1] BRAY F, FERLAY J, SOERJOMATARAM I, SIEGEL RL, TORRE LA et al. Global cancer statistics 2018: GLOBOCAN estimates of incidence and mortality worldwide for 36 cancers in 185 countries. CA Cancer J Clin 2020; 70: 313. https://doi.org/10.3322/caac.21609

[2] NASIM F, SABATH BF, EAPEN GA. Lung Cancer. Med Clin North Am 2019; 103: 463–473. https://doi.org/10.1016/j.mcna.2018.12.006

[3] CAO M, CHEN W. Epidemiology of lung cancer in China. Thorac Cancer 2019; 10: 3–7. https://doi.org/10.1111/1759-7714.12916

[4] HIRSCH FR, SCAGLIOTTI GV, MULSHINE JL, KWON R, CURRAN WJ JR et al. Lung cancer: current therapies and new targeted treatments. Lancet 2017; 389: 299–311. https://doi.org/10.1016/S0140-6736(16)30958-8

[5] HERBST RS, MORGENSZTERN D, BOSHOFF C. The biology and management of non-small cell lung cancer. Nature 2018; 553: 446–454. https://doi.org/10.1038/nature25183

[6] JONES GS, BALDWIN DR. Recent advances in the management of lung cancer. Clin Med (Lond) 2018; 18: s41–s46. https://doi.org/10.7861/clinmedicine.18-2-s41

[7] RUIZ-CORDERO R, DEVINE WP. Targeted Therapy and Checkpoint Immunotherapy in Lung Cancer. Surg Pathol Clin 2020; 13: 17–33. https://doi.org/10.1016/j.path.2019.11.002

[8] ZHOU WY, CAI ZR, LIU J, WANG DS, JU HQ et al. Circular RNA: metabolism, functions and interactions with proteins. Mol Cancer 2020; 19: 172. https://doi.org/10.1186/s12943-020-01286-3

[9] CHEN LL, YANG L. Regulation of circRNA biogenesis. RNA Biol 2015; 12: 381–388. https://doi.org/10.1080/15476286.2015.1020271

[10] ZANG J, LU D, XU A. The interaction of circRNAs and RNA binding proteins: An important part of circRNA maintenance and function. J Neurosci Res 2020; 98: 87–97. https://doi.org/10.1002/jnr.24356

[11] HANSEN TB, KJEMS J, DAMGAARD CK. Circular RNA and miR-7 in cancer. Cancer Res 2013; 73: 5609–5612. https://doi.org/10.1158/0008-5472.CAN-13-1568

[12] VERDUCI L, STRANO S, YARDEN Y, BLANDINO G. The circRNA-microRNA code: emerging implications for cancer diagnosis and treatment. Mol Oncol 2019; 13: 669–680. https://doi.org/10.1002/1878-0261.12468

[13] LIU P, WU D, DUAN J, XIAO H, ZHOU Y et al. NRF2 regulates the sensitivity of human NSCLC cells to cystine deprivation-induced ferroptosis via FOCAD-FAK signaling pathway. Redox Biol 2020; 37: 101702. https://doi.org/10.1016/j.redox.2020.101702

[14] QU S, ZHONG Y, SHANG R, ZHANG X, SONG W et al. The emerging landscape of circular RNA in life processes. RNA Biol 2017; 14: 992–999. https://doi.org/10.1080/15476286.2016.1220473

[15] LI B, ZHU L, LU C, WANG C, WANG H et al. circNDUFB2 inhibits non-small cell lung cancer progression via destabilizing IGF2BPs and activating anti-tumor immunity. Nat Commun 2021; 12: 295. https://doi.org/10.1038/s41467-020-20527-z

[16] ZHANG N, NAN A, CHEN L, LI X, JIA Y et al. Circular RNA circSATB2 promotes progression of non-small cell lung cancer cells. Mol Cancer 2020; 19: 101. https://doi.org/10.1186/s12943-020-01221-6

[17] XIAO H, ZHAO R, MENG W, LIAO Y. Effects and translatomics characteristics of a small-molecule inhibitor of METTL3 against non-small cell lung cancer. J Pharm Anal 2023; 13: 625–639. https://doi.org/10.1016/j.jpha.2023.04.009

[18] YIN H, CHEN L, PIAO S, WANG Y, LI Z et al. M6A RNA methylation-mediated RMRP stability renders proliferation and progression of non-small cell lung cancer through regulating TGFBR1/SMAD2/SMAD3 pathway. Cell Death Differ 2023; 30: 605–617. https://doi.org/10.1038/s41418-021-00888-8

[19] QIU FS, HE JQ, ZHONG YS, GUO MY, YU CH. Implications of m6A methylation and microbiota interaction in non-small cell lung cancer: From basics to therapeutics. Front Cell Infect Microbiol 2022; 12: 972655. https://doi.org/10.3389/fcimb.2022.972655

[20] LI X, FANG J, TAO X, XIA J, CHENG B et al. Splice site m(6)A methylation prevents binding of DGCR8 to suppress KRT4 pre-mRNA splicing in oral squamous cell carcinoma. Peer J 2023; 11: e14824. https://doi.org/10.7717/peerj.14824

[21] WANG X, MA R, ZHANG X, CUI L, DING Y et al. Crosstalk between N6-methyladenosine modification and circular RNAs: current understanding and future directions. Mol Cancer 2021; 20: 121. https://doi.org/10.1186/s12943-021-01415-6

[22] CHEN C, YUAN W, ZHOU Q, SHAO B, GUO Y et al. N6-methyladenosine-induced circ1662 promotes metastasis of colorectal cancer by accelerating YAP1 nuclear localization. Theranostics 2021; 11: 4298–4315. https://doi.org/10.7150/thno.51342

[23] LI Z, YANG HY, DAI XY, ZHANG X, HUANG YZ et al. CircMETTL3, upregulated in a m6A-dependent manner, promotes breast cancer progression. Int J Biol Sci 2021; 17: 1178–1190. https://doi.org/10.7150/ijbs.57783

[24] HONG W, XUE M, JIANG J, ZHANG Y, GAO X. Circular RNA circ-CPA4/ let-7 miRNA/PD-L1 axis regulates cell growth, stemness, drug resistance and immune evasion in non-small cell lung cancer (NSCLC). J Exp Clin Cancer Res 2020; 39: 149. https://doi.org/10.1186/s13046-020-01648-1

[25] LIU M, FAN Y, LI D, HAN B, MENG Y et al. Ferroptosis inducer erastin sensitizes NSCLC cells to celastrol through activation of the ROS-mitochondrial fission-mitophagy axis. Mol Oncol 2021; 15: 2084–2105. https://doi.org/10.1002/1878-0261.12936

[26] HUANG J, DENG C, GUO T, CHEN X, CHEN P et al. Cinobufotalin Induces Ferroptosis to Suppress Lung Cancer Cell Growth by lncRNA LINC00597/hsa-miR-367-3p/TFRC Pathway via Resibufogenin. Anticancer Agents Med Chem 2023; 23: 717–725. https://doi.org/10.2174/1871520622666221010092922

[27] ZHANG H, GE Z, WANG Z, GAO Y, WANG Y et al. Circular RNA RHOT1 promotes progression and inhibits ferroptosis via mir-106a-5p/STAT3 axis in breast cancer. Aging (Albany NY) 2021; 13: 8115–8126. https://doi.org/10.18632/aging.202608

[28] WANG HH, MA JN, ZHAN XR. Circular RNA Circ_0067934 Attenuates Ferroptosis of Thyroid Cancer Cells by miR-545-3p/SLC7A11 Signaling. Front Endocrinol (Lausanne) 2021; 12: 670031. https://doi.org/10.3389/fendo.2021.670031

[29] SHANSHAN W, HONGYING M, JINGJING F, YIMING Y, YU R et al. CircDTL Functions as an Oncogene and Regulates Both Apoptosis and Ferroptosis in Non-small Cell Lung Cancer Cells. Front Genet 2021; 12: 743505. https://doi.org/10.3389/fgene.2021.743505

[30] WU J, MINIKES AM, GAO M, BIAN H, LI Y et al. Intercellular interaction dictates cancer cell ferroptosis via NF2-YAP signalling. Nature 2019; 572: 402–406. https://doi.org/10.1038/s41586-019-1426-6

[31] LU Y, YANG Q, SU Y, JI Y, LI G et al. MYCN mediates TFRC-dependent ferroptosis and reveals vulnerabilities in neuroblastoma. Cell Death Dis 2021; 12: 511. https://doi.org/10.1038/s41419-021-03790-w

[32] YIN TF, ZHAO DY, ZHOU YC, WANG QQ, YAO SK. Identification of the circRNA-miRNA-mRNA regulatory network and its prognostic effect in colorectal cancer. World J Clin Cases 2021; 9: 4520–4541. https://doi.org/10.12998/wjcc.v9.i18.4520

[33] DATTILO D, DI TIMOTEO G, SETTI A, GIULIANI A, PERUZZI G et al. The m(6)A reader YTHDC1 and the RNA helicase DDX5 control the production of rhabdomyosarcoma-enriched circRNAs. Nat Commun 2023; 14: 1898. https://doi.org/10.1038/s41467-023-37578-7

[34] LUO J, LIU L, SHEN J, ZHOU N, FENG Y et al. miR5765p promotes epithelialtomesenchymal transition in colorectal cancer by targeting the Wnt5amediated Wnt/betacatenin signaling pathway. Mol Med Rep 2021; 23. https://doi.org/10.3892/mmr.2020.11733

[35] ZHANG L, CHEN J, WANG L, CHEN L, DU Z et al. LincPINT acted as a tumor suppressor by sponging miR-543 and miR-576-5p in esophageal cancer. J Cell Biochem 2019; 120: 19345–19357. https://doi.org/10.1002/jcb.28699

[36] NI XF, ZHAO LH, LI G, HOU M, SU M et al. MicroRNA-548-3p and MicroRNA-576-5p enhance the migration and invasion of esophageal squamous cell carcinoma cells via NRIP1 down-regulation. Neoplasma 2018; 65: 881–887. https://doi.org/10.4149/neo_2018_171206N803

[37] ZHOU J, WANG L, SUN Q, CHEN R, ZHANG C et al. Hsa_circ_0001666 suppresses the progression of colorectal cancer through the miR-576-5p/PCDH10 axis. Clin Transl Med 2021; 11: e565. https://doi.org/10.1002/ctm2.565

[38] ZOU H, MAO Q. Circ_0037078 promotes trophoblast cell proliferation, migration, invasion and angiogenesis by miR-576-5p/IL1RAP axis. Am J Reprod Immunol 2022; 87: e13507. https://doi.org/10.1111/aji.13507

[39] MA Q, WANG X, LI J. LncRNA RP1-86C11.7 exacerbates the glioma progression and oncogenicity by hsa-miR-144-3p/TFRC signaling. Transl Oncol 2021; 14: 101215. https://doi.org/10.1016/j.tranon.2021.101215

[40] CUI P, DAI X, LIU R, CAO H. LncRNA LINC00888 upregulation predicts a worse survival of laryngeal cancer patients and accelerates the growth and mobility of laryngeal cancer cells through regulation of miR-378g/TFRC. J Biochem Mol Toxicol 2021; 35: e22878. https://doi.org/10.1002/jbt.22878